Water and Polymer Dynamics in Chemically Cross-Linked Hydrogels of Poly(vinyl alcohol): A Molecular Dynamics Simulation Study

Ester Chiessi,* Francesca Cavalieri, and Gaio Paradossi

Dipartimento di Scienze e Tecnologie Chimiche, University of Rome Tor Vergata, Via della Ricerca Scientifica, 00133 Rome, Italy

Received: October 30, 2006; In Final Form: January 18, 2007

A topologically extended model of a chemically cross-linked hydrogel of poly(vinyl alcohol) (PVA) at high hydration degree has been developed for a molecular dynamics simulation with atomic detail at 323 K. The analysis of the 5 ns trajectory discloses structural and dynamic aspects of polymer solvation and elucidates the water hydrogen bonding and diffusion in the network. The features of local polymer dynamics indicate that PVA mobility is not affected by structural constraints of chemical junctions at the investigated cross-linking density, with a prevailing dumping effect due to water interaction. Simulation results are validated by a favorable comparison with findings of an incoherent quasi-elastic neutron scattering study of the same hydrogel system.

1. Introduction

A large amount of scientific works in recent literature deals with investigations on hydrogel systems, spanning from the search of new scaffold materials and preparation methods[1−4] to the molecular characterization of the structure and dynamics of the system components.[5−11] Hydrogels belong to the current technology, with applications in the agricultural, cosmetic, pharmaceutical, and food industry. In many of these applications, the solid-like character of the hydrogel system plays an important role, providing a mechanical stability to the system that, however, maintains an intrinsic dynamic behavior typical of liquid phases. Hydrogel matrixes can allow both nonreactive processes, such as diffusion of drugs, gases, metabolites,[12−15] and chemical reactions, as in hydrogel supported enzymatic catalysis.[16−17]

In a recent paper, the hypothesis has been proposed that the first cell(s) on the Earth assembled in a hydrogel matrix, which could provide a stable environment not only for the accretion of polymeric mass, but also for subsequent cell division and evolution.[18] These ideas seem to support the concept of using hydrogels in medicine as soft living matter, which, envisaged for their potential use up to two decades ago, are now becoming a real chance for new therapeutic approaches[19] and for tissue engineering and substitution.[20−21]

The functionality of the hydrogel system depends on both its structural and its dynamic properties. Structural aspects of the organic moiety (often a polymeric material) concern conformations, physical and/or chemical junctions, mesh size, moving to increasing space domains, and the "structuring"/"destructuring" effect on water molecules is a peculiar feature of hydrogel systems, due to the interaction of solvent with the hydrophyllic/hydrophobic organic components.[22] Water and polymer dynamics are strictly related to the molecular structure of the hydrogel, and they are essential in processes involving permeability, adhesion, and responsivity, requirements often invoked in biomedical applications of hydrogel matrixes.[23] In this respect, it could be argued that the dynamics of the molecular components of the hydrogel greatly affects the kinetics of nonreactive phenomena that can occur in the matrix, such as diffusion of penetrants or conformational rearrangements of embedded macromolecules;[24] therefore, a complete characterization of the system should involve both the dynamic behavior of water, the main constituent of biological hydrogels, and of the polymeric moiety. This analysis implies to explore a time window of several decades from picoseconds to tenths of seconds.

The molecular dynamics (MD) method has been applied in the past decade in simulation studies of polymer dynamics in melts and bulk networks employing bead-spring models for monomers.[25−27] Classical MD simulations of polymer solutions, including an explicit molecular description of solvent and solute, are scarce, due to the heavy expense of computing resources as the system size for a correct sampling is large and the acquired time has to be long for a complete relaxation of the dynamic processes.[28−35] In particular, classical MD investigations of chemical hydrogels with a high water content are, to our knowledge, lacking, although the gain of information on polymer−water interactions resulting from this approach is alluring.

From an experimental point of view, incoherent quasi-elastic neutron scattering (QENS) represents a proper approach to elucidate water dynamical properties. Moreover, polymer dynamics can be assessed with the same technique in D_2O swollen systems. MD simulations provide a modeling counterpart to QENS, exploring both methods' time and space windows of picoseconds and Ångstroms, respectively. Matching of experimental to theoretical results yields a view of the system at a molecular level, giving confidence to the predictive potentialities of the simulation for the formulation of novel hydrogels.

The concerted approach of QENS and MD investigations has been recently adopted by us in the study of chemically cross-linked hydrogels of poly(vinyl alcohol) (PVA).[36−37] These soft matrixes, under scrutiny in our laboratory for biomedical applications, such as *in situ* drug delivery and tissue engeneering,[38−39] are formed by a polymeric network of self-cross-linked

* To whom correspondence should be addressed: ester.chiessi@uniroma2.it.

10.1021/jp0671143 CCC: $37.00
Published on Web 02/27/2007

PVA chains and display a water content that can achieve up to 90% (w/w), depending on polymerization degree and concentration of the polymer in the starting solution prior to the cross-linking reaction. A supercooling effect on water in PVA chemical hydrogels has been evidenced by QENS measurements,[36] and in a previous work, we have evaluated the solvent diffusion parameters in a MD study of the junction zone of the hydrogel, with a good agreement to experimental results.[37]

The present paper reports on a MD investigation of PVA chemical hydrogels with the aim to explore the local polymer dynamics on a time scale of nanoseconds. An extended model of the network, including several chemical junctions, has been developed, where the topological constraints and the percolation of the polymeric scaffold have been taken into account. By increasing the space and time domains of the simulated system, in comparison to the previous study,[37] we were able to examine some dynamic properties of the polymeric scaffold and to have a clearer and more realistic picture of the polymer-induced modification of the water dynamics in the hydrogel.

2. Methods

2.1. Developing the Model. The chemical hydrogels studied in the present work are prepared by the acetalization reaction of telechelic PVA chains, i.e., linear chains bearing two terminal aldehyde groups, in aqueous solution.[40] The network resulting from this self-cross-linking process is formed by three-functional junctions that connect chains with an average degree of polymerization (DP) related to that of the starting telechelic chains. For an average DP of the PVA telechelic equal to N, one should expected an average DP of $N/2$ for chains between cross links, if every chain end of the telechelic chains has been effective in the propagation of the network. Taking into account that aldehyde groups are able to react in an intramolecular fashion producing dangling ends, which are inactive in the networking process, chains with a DP higher than $N/2$ could be involved in the final structure of the network.

PVA hydrogel samples investigated by QENS measurements[36] and here simulated have been prepared by PVA telechelic with a number-average molecular weight of 2000 g/mol, corresponding to an average DP of about 46 monomer per chain. A dynamic mechanical analysis allowed us to experimentally evaluate the characteristic parameters of the network, and values of 4.4×10^{-5} mol/cm^3 and 3000 g/mol have been determined for the chain density in the swollen system, ρ_h, and the number-average molecular weight between cross links, M_c, respectively, in a hydrogel matrix with 90% (w/w) of water and a polymer volume fraction, Φ_2, of 0.12.[36] The M_c value corresponds to an average DP of 68 monomer per chain.

These hydrogel properties have been considered to formulate a realistic model of the system in the simulation. The starting scaffold of the polymeric network has been built by three linear PVA chains (named A, B, C) in a fully extended conformation, each of 140 residues, arranged in the simulation box with a parallel orientation with respect to the Cartesian axes and by three 69 residues linear chains (D, E, F) acting as cross linkers of the main chains. The resulting topology is schematically shown in Chart 1.

The polymer has then been hydrated with a shell of water of thickness suited to introduce a water content corresponding to the experimental Φ_2, and the system has been compressed to the correct final density by means a preliminary MD simulation applying a "pressure bath" of 1 atm with the Berendsen's pressure coupling algorithm. At this stage, a covalent bond between the last carbon atom and the nearest periodic image of the first carbon atom of the chain has been added in the force field for the A, B, and C chains, aiming to simulate an isotropic covalent percolation of the network. After energy minimization, the system has been equilibrated in 750 ps of MD at constant volume and 323 K. The following trajectory has been considered as production run. In the final configuration, the simulation box contained 6 chemical junctions connecting 9 PVA chains with DP 69 and 8773 water molecules, for a chain density of 5×10^{-5} mol/cm^3.

CHART 1: Network Model

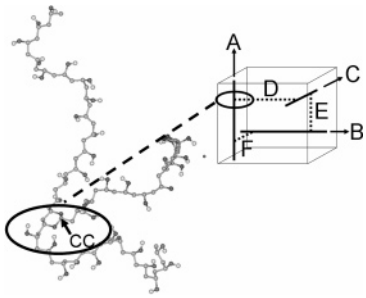

2.2 Simulation Details. Calculations have been performed on an IBM Linux Cluster 1350 at the CINECA Supercomputing Center (Bologna, Italy).

The GROMACS force field with the united atom convention for CH and CH_2 groups has been used. The 1,3-dioxane six-member ring of the junctions (see Chart 1) has been treated as already reported,[37] and water has been simulated by the single-point charged (SPC) intermolecular potential model.[41] MD simulations have been performed by GROMACS software, version 3.2.1.[42−43]

Equilibration and production runs have been carried out in the *NVT* ensemble, with the leapfrog integration algorithm[44] using a time step of 0.5 fs. Temperature has been controlled at 323 K by the Berendsen's temperature coupling algorithm.[45] Nonbonding interactions have been treated as described in a previous work.[37]

The total simulation time, including equilibration, was 5.2 ns. The configurations were saved every 0.1 ps.

A water box of 10 019 molecules with the same size of the hydrogel model was considered to simulate bulk water properties for a comparison. A total trajectory of 400 ps has been calculated for the water box at 323 K.

3. Results and Discussion

3.1. Polymer−Water Interaction and Water Dynamics. The study of PVA-telechelic hydrogels by QENS evidenced the presence of a component of slow relaxing water, which displays a "random-jump" diffusion behavior with diffusion coefficient lower than the corresponding bulk water value.[36] In the present work, we have investigated the polymer−solvent interaction and characterized this supercooled water in the simulated system, evaluating the water diffusional properties with an approach similar to that already applied in the study of the junction zone of the hydrogel.[37]

The water distribution in the polymer network can be investigated by means of radial distribution functions, $g_{A-B}(r)$, where A and B are PVA and water atoms, respectively. The $g_{A-B}(r)$ function gives the local density of atoms B around atoms A at a distance r, divided by the average density considering the whole system. In a homogeneous system, the $g_{A-B}(r)$ value approaches unity at large distances, but this feature may not be expected in systems where a clustering of solute is present. This

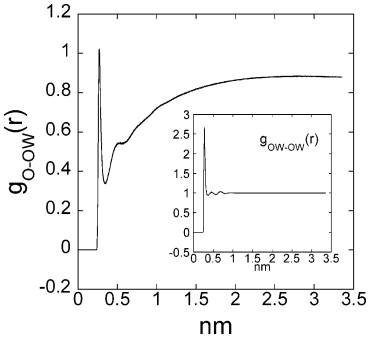

Figure 1. Radial distribution function of PVA oxygens with water oxygens. Inset: radial distribution function of water oxygens in bulk water.

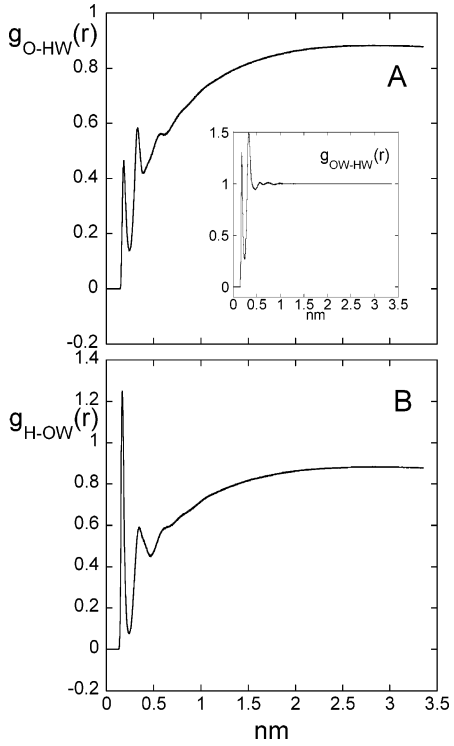

Figure 2. (A) Radial distribution function of PVA oxygens with water hydrogens and radial distribution function of oxygens with hydrogens in bulk water (inset). (B) Radial distribution function of PVA hydrogens with water oxygens.

effect has been observed in a very pronounced fashion in MD simulations of hydrated membranes.[46]

The radial distribution function between PVA and water oxygen atoms, $g_{O-OW}(r)$ (Figure 1) shows the effect of the polymer−water interaction on the solvation pattern of the PVA hydroxylic groups. It can be noted that the $g_{O-OW}(r)$ value remains lower than unity (about 0.9) also at large distances for the occurrence of entanglements and small-sized clusters, according to the experimental evidence of a propensity of PVA to form aggregated micro-domains in hydrogels.[47] The same $g(r)$ behavior is observed in Figure 2 and in the radial distribution function of water around the network junctions. This feature has been taken into account for the evaluation of the coordination numbers.

The maximum of $g_{O-OW}(r)$ at 0.28 nm suggests a hydrogen bond regime in the first hydration shell of PVA hydroxylic groups, and an average coordination number, n_{O-OW}, of 1.9 water oxygens per PVA oxygen can be evaluated by integration:

$$n_{O-OW} = \frac{N_{OW}}{V}\int_0^{R_{min}} 4\pi r^2 g_{O-OW}(r)\,dr \quad (1)$$

where N_{OW} and R_{min} are the number of water molecules in the simulation box of volume V and the first minimum distance in $g_{O-OW}(r)$, respectively.

The hydrogen bond (HB) between PVA hydroxylic groups and water has been studied by analyzing the trajectory for the occurrence of this interaction, adopting as geometric criteria an acceptor−donor distance (A···D) lower than 0.3 nm and an angle Θ (A···H−D) higher than 120°. On average, 1.2 ± 0.1 hydrogen bonds per PVA residue were found.

HBs formed by a polymer OH group acting as a H acceptor and HBs formed by an OH group acting as a H donor have been separately evaluated by integration of the radial distribution functions between PVA oxygen and water hydrogen atoms, $g_{O-HW}(r)$, and between PVA hydrogen and water oxygen atoms, $g_{H-OW}(r)$, respectively, shown in Figure 2. In eq 2 and 3

$$n_{ACC} = \frac{N_{HW}}{V}\int_0^{R_{min}} 4\pi r^2 g_{O-HW}(r)\,dr = 0.75 \pm 0.02 \quad (2)$$

$$n_{DO} = \frac{N_{OW}}{V}\int_0^{R_{min}} 4\pi r^2 g_{H-OW}(r)\,dr = 0.61 \pm 0.02 \quad (3)$$

n_{ACC} and n_{DO} are the average number of HBs formed as acceptor and donor per PVA hydroxylic group, respectively.

From an inspection of Figures 1 and 2, it can be noted that the perturbation of the water distribution around PVA hydroxylic groups, relative to the average water density, extends to a radius of about 2 nm from the polymer. The comparison with the radial distribution functions in bulk water, shown in the inset of Figure 1 and 2A, indicates a less structured coordination of PVA hydroxylic groups with respect to that observed in bulk water.

The $g_{O-OW}(r)$ in Figure 1 is similar to that reported in the previous work on the junction zone of the hydrogel.[37] A higher average coordination number n_{O-OW} was obtained using a model of reduced size and a simpler topology.[37] The difference, i.e., 2.2 instead of 1.9, reflects a lower average accessibility of the polymer, which forms locally aggregated domains and entanglements in the more realistic network model adopted in the present work.

In order to select the water according to the interactions with polymer chains, we sampled the solvent in different domains, according to the $g_{O-OW}(r)$ behavior of Figure 1. A "close contact" domain (I) was defined, including water molecules at a distance lower than 0.6 nm. Water at distances between 0.6 and 2 nm, where the perturbation in the $g_{O-OW}(r)$ is minor, was chosen as a second domain (II); the remaining water molecules were considered in a last domain (III). Solvent in domains I, II, and III has been characterized in terms of a diffusion coefficient and residence time in a diffusion site.

The water diffusion coefficient, D, has been obtained from the long-time slope of the mean square displacement:

$$D = \frac{1}{6}\lim_{t\to\infty}\frac{d}{dt}\langle|\mathbf{r}(t) - \mathbf{r}(0)|^2\rangle \quad (4)$$

where $\mathbf{r}(t)$ and $\mathbf{r}(0)$ correspond to the position vector of the water oxygen at time t and 0, respectively, with an average performed over both time origins and water molecules. To evaluate the limiting slope, we considered a time window equal to the average lifetime of the hydrogen bonds (HB) between PVA hydroxylic groups and water. The time evolution of this interaction is shown in Figure 3, where the time autocorrelation

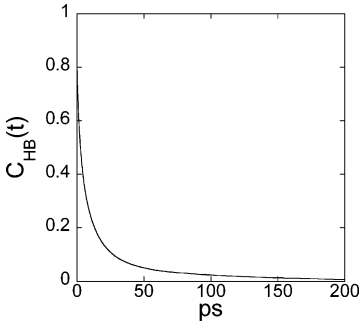

Figure 3. Decay of the autocorrelation function $C_{HB}(t)$ of hydrogen bonds between PVA hydroxylic groups and water.

TABLE 1: Ratio between Diffusion Coefficient of Water Molecules of Different Domains in the Hydrogel, *D*, and Diffusion Coefficient of Bulk Water, D_0

	I domain	II domain	III domain	QENS[a]
D/D_0	0.64 ± 0.05	0.96 ± 0.08	1.04 ± 0.09	0.68 ± 0.06

[a] Experimental diffusion coefficient,[36] normalized to the diffusion coefficient of bulk water.[48]

TABLE 2: Water Hydrogen Bond Properties in Different Domains of PVA Hydrogel

	I domain	II domain	III domain	bulk
HB number per water molecule	1.3 ± 0.1	1.4 ± 0.1	1.2 ± 0.1	1.2 ± 0.1
τ_{HB} (ps)	2.0 ± 0.1	1.6 ± 0.1	1.6 ± 0.1	1.3 ± 0.1

function of the hydrogen bonds, $C_{HB}(t)$, is reported. The correlation time, t^*, obtained by integrating $C_{HB}(t)$ in a range of about $20t^*$, is 10.5 ± 0.5 ps, and the last value was used as an estimate of the average lifetime of the HB interaction, which can be considered as the highest limiting value for the belonging time in a particular domain of a water molecule. In Table 1, the D/D_0 ratio, where D_0 is the diffusion coefficient of bulk water, is reported for each water domain, to be compared with the D/D_0 value obtained by QENS measurements. The best agreement between the experimental and calculated results observed for the water in domain I seems to identify the supercooled water component in the PVA hydrogel with the solvent in a surrounding of 0.6 nm from the polymer. It follows that, in spite of the high hydration degree of the system (85% w/w), about 30% of water in the system is dynamically quenched.

The structure and dynamics of HBs involving water molecules in different domains have been analyzed, and the results are summarized in Table 2. The average number of HBs per water molecules (including also HBs with PVA hydroxylic groups for water in domain I) is about 1.3, irrespective of the domain. A similar value, within errors, is found for bulk water. This evidence suggests that the polymer interaction does not significantly affect the HB connectivity between water molecules, whereas HB dynamics is influenced with an increase of the HB autocorrelation time τ_{HB} of about 50% in domain I and of about 25% in domain II, in comparison with bulk water, as reported in Table 2 and shown in Figure 4. It is noteworthy that the effect of lifetime increasing for the HB interaction of water in the first hydration shell of PVA hydroxylic groups (with τ^* of about 10 ps, Figure 3) strongly propagates to water molecules not directly in contact with the polymer within domain I (with τ_{HB} of 2.0 ps) and also, in a minor extent, to all water molecules in the hydrogel.

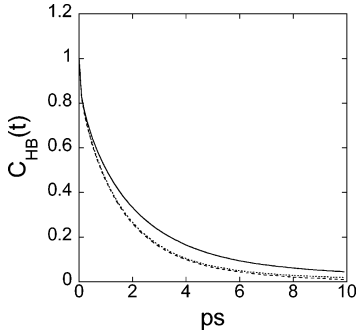

Figure 4. Decay of the HB autocorrelation function $C_{HB}(t)$ between water molecules in different domains of the hydrogel: (—) water molecules with a distance from PVA lower than 0.6 nm; (··· ····) water molecules with a distance from PVA between 0.6 and 2 nm; (---) water molecules with a distance from PVA higher than 2 nm.

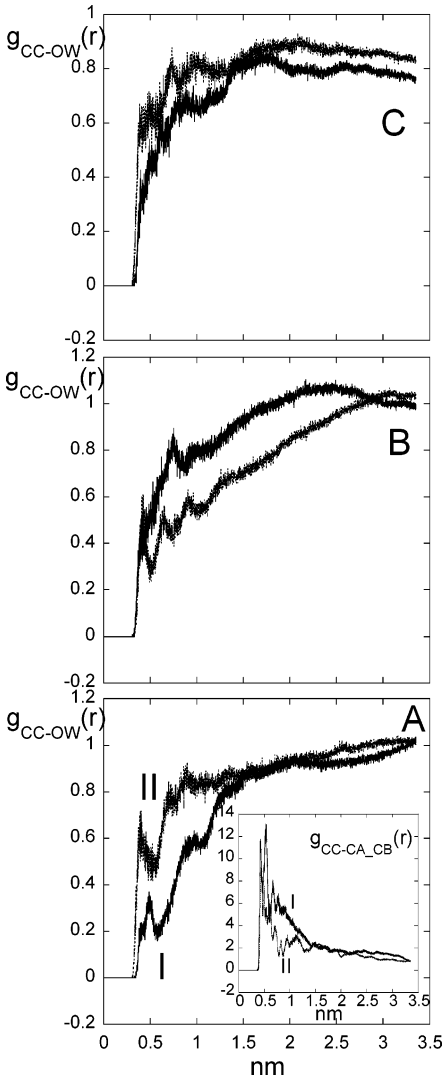

Figure 5. Radial distribution function of the junction carbon atom labeled CC in Chart 1 with water oxygens. (A) CC atoms of chain A in Chart 1. (B) CC atoms of chain B in Chart 1. (C) CC atoms of chain C in Chart 1. Inset of (A): radial distribution function of CC atoms of chain A in Chart 1 with PVA carbon atoms.

Solvation of junction zones of the polymer network can be described by considering the radial distribution functions $g_{CC-OW}(r)$ between the acetal carbon, labeled as CC in Chart 1, of each junction and water oxygen atoms. Figure 5 shows the six $g_{CC-OW}(r)$ functions, calculated for the last 400 ps trajectory. Excluded volume effects on the solvation pattern

extend to a distance of about 1.5/2.5 nm, with a certain heterogeneity between junction domains that is maintained during the trajectory. The radial distribution function between PVA chain carbon atoms and the CC junction atom, $g_{CC-CA\_CB}(r)$ (CA, CB referring to methylene, methyne groups) displays a complementary behavior to the corresponding $g_{CC-OW}(r)$, as shown in the inset of Figure 5A for two junctions. It can be noted that regions with a lower water density around the junction have a corresponding higher polymer density.

Dynamics of HBs between water molecules in the surrounding of the junctions is quenched, as indicated by the average τ_{HB} , $<\tau_{HB}>$, of 2.1 ± 0.2 ps calculated including water in a radius of 1 nm from CC atoms. QENS experiments allowed to evaluate the residence time τ_r of a bulk water molecule in a diffusion site, together with the diffusion coefficient.[49] By the same method, we obtained a τ_r of 2.4 ± 0.2 ps for the slow component of water in PVA telechelic hydrogels at 323 K[36], which compares favorably with the HB autocorrelation times calculated for water molecules in domain I (Table 2) and in the surrounding of the junction ($<\tau_{HB}>$).

From a comparison of the results about water dynamics in PVA telechelic hydrogels obtained in the present work, using a topologically extended model of the polymer network, and in the previous work, where a single junction zone of the system was simulated,[37] we note that a marked difference emerges in the extent of the polymer-induced supercooling effect. Under similar conditions of polymer concentration, in the present model, about 30% of the solvent in the hydrogel displays a slower diffusivity, to be compared to a value of 8% obtained in the previous study, where only water molecules of the first solvation shell ensued dynamically quenched.[37] An evaluation of the relative quantity of "slow" and "fast" water in PVA hydrogels by QENS is not available, as the scattering contribution of "bulk"-type water often falls within the background of the signal, and the slow to fast water amount ratio is not quantitatively accessible. Taking into account that PVA telechelic chains form stable "wall-to-wall" hydrogel samples with a high resistance to mechanical deformations,[40] it can be expected that the structural cohesion of the system due to the polymeric scaffold is enhanced by a considerable water involvement, probably well beyond the water of the first hydration shell as in a polymer solution.

Another difference in comparison with the results of the simulation of the hydrogel junction[37] is found in the lifetime τ^* of HBs between PVA hydroxylic groups and water molecules. In the present work, a τ^* value of 10.5 ± 0.5 ps has been obtained, about twice that reported in the former paper[37] at 323 K. A greater slowering of water in the HB interaction with PVA, as indicated by the higher τ^* value, is consistent with the result of a higher fraction of supercooled water in the system.

On the basis of these considerations, the hydrogel model adopted in the present work seems to provide a more realistic description of the dynamic behavior of the molecular components in the system. The long-range effect on water dynamics can be evidenced when at least a complete network cage is included in the model, i.e., the confining element of the solvent is explicitly introduced, suggesting the presence of cooperative effects in the polymer−solvent interaction.

3.2. Conformational and Segmental Dynamics of PVA. The QENS technique can explore a space-time domain corresponding to a few Ångstroms and up to hundreds of picoseconds, respectively. An analysis of the polymer dynamics within this resolution focuses the local segmental mobility and in the case of PVA relates to polymer sequences of 5/10 chain residues. A key element of this mobility is the torsional dynamics of the backbone, governed by the possibility of transitions between different conformations of the chain dihedral angles. In a PVA chain, the dihedral angles defined by the backbone carbon atoms are all equivalent; therefore, a description of the polymer conformation in the hydrogel network can be performed in term of a single dihedral angle θ, by considering two dihedrals per residue except the five residues nearest to the junction. Figure 6 shows the distribution $P(\theta)$ calculated along the whole trajectory and the relative free energy, $G(\theta) - G(180)$, obtained as

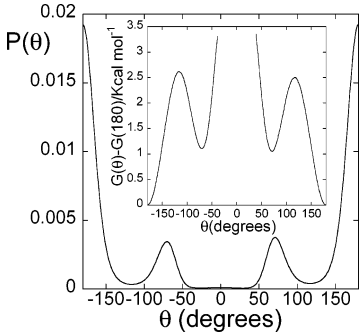

Figure 6. Backbone dihedral angles distribution. Inset: relative free energy, calculated by eq 5.

$$G(\theta) - G(180) = -RT \ln \frac{P(\theta)}{P(180)} \tag{5}$$

where $\theta = 180°$ corresponds to the trans conformation, the most populated conformational state. According to the atacticity of telechelic PVA,[36] the gauche states (g and g^*, $\theta = \pm 70°$) have equal probability and have free energies approximately 1.1 kcal/mol above the trans state. The cis state is practically not populated. We have monitored the backbone dihedrals throughout the simulation to detect the transitions between rotational states. The transitions occur between the trans state and one of the gauche states, as the cis barrier has been never crossed during our simulation.

An average lifetime of rotational state, $<\tau_{rot}>$, of 161 ps has been estimated by means of eq 6:

$$\langle \tau_{rot} \rangle = \frac{1}{N_{DIHE}} \sum_{i=1}^{N_{DIHE}} \frac{t_{TOT}}{(N_{TRANS,i} + 1)} \tag{6}$$

where N_{DIHE}, t_{TOT}, and $N_{TRANS,i}$ are the number of dihedral angles that perform transitions, the total simulation time, and the number of transitions of the i-th dihedral angle, respectively. In eq 6, the single term of the summation represents the time-average lifetime of a rotational state for the i-th dihedral angle, $\tau_{rot,i}$; then, the average is performed on mobile chain dihedral angles. The torsional dynamic behavior of PVA in the polymer network is quite heterogeneous. About 25% of dihedral angles do not undergo any transition, about 40% have a rotational lifetime between 550 and 110 ps, and about 14% have a rotational lifetime shorter than 50 ps. This dynamic heterogeneity is not related to the position of the dihedral in the chain with respect to a junction and can be expressed by the standard deviation of $\tau_{rot,i}$ corresponding to the average of eq 6, which amounts to about one hundred picoseconds. An analysis of dihedral angle distribution and isomerization dynamics of PVA has been reported in a MD study of a PVA 15-mer in solution at 300 K.[33] In the case of a water solution with $\Phi_2 = 0.07$, the

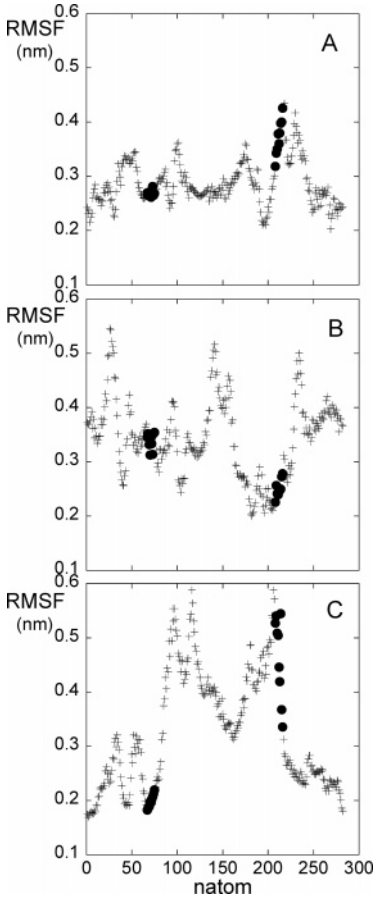

Figure 7. Root mean squared fluctuation (RMSF) of atomic positions for PVA carbon atom as a function of the atom location along the polymer chain: (+) PVA carbon atoms between junctions; (●) PVA junction atoms.

population of the rotational states is similar to that found in the present work, whereas the average conformational transition rate, after correction for the difference in temperature, is quite lower. This comparison seems to indicate that the local conformational behavior of PVA in the network at the investigated degree of swelling is not further influenced by the presence of chemical junctions.

At the aim to evaluate the local mobility of PVA in the hydrogel network, the root mean squared fluctuation (RMSF) of atomic positions for each carbon atom has been determined:

$$\mathrm{RMSF}_i = \sqrt{\langle(\mathbf{r}_i(t) - \langle\mathbf{r}_i\rangle)^2\rangle_t} \tag{7}$$

The results are shown in Figure 7, where RMSFs are reported as a function of the atom location along the polymer chain for the three percolating chains (see Chart 1). Full symbols indicate atoms belonging to the network junctions. Fluctuations range from 0.2 to 0.6 nm, with an average of about 0.4 nm. It should be noted that regions with a higher mobility can be found both in the middle of a strand and in the proximity of a junction. A similar independence of mobility by position in chain has been reported for PVA in aqueous solution, where no enhancement in the mobility has been noted at the chain ends.[33] It could be argued that the interaction with water induces a dumping effect on the local dynamics of PVA network chains, hiding the influence of topological restraints.

Results of QENS experiments on telechelic PVA hydrogels, performed after a complete replacement of water with D_2O, indicate a constrained diffusion regime for the polymer segmental dynamics.[36] A characteristic well dimension of 0.9 ± 0.1 nm has been evaluated, and a residence time of an average chain segment in a local conformation of 150 ± 20 ps has been estimated at 323 K.[36] MD results are in good agreement with QENS experimental data, with a well dimension from the simulation of 0.8 nm, i.e., 2·<RMSF>, and a residence time, estimated as average rotational lifetime, of 161 ps.

In addition, we have investigated the behavior of the orientational autocorrelation function (OACF) of C−O vectors of PVA, given as

$$P_{\mathrm{C-O}}(t) = \frac{1}{2}\left[3\cdot\langle|\mathbf{e}(t)\cdot\mathbf{e}(0)|^2\rangle - 1\right] \tag{8}$$

where $\mathbf{e}(t)$ is a unit vector and < > denotes an ensemble average over all C−O vectors located at least ten residues from the junctions. The decay of OACF can be adequately described by a stretched exponential or a Kohlrausch−Williams−Watts (KWW) expression given by

$$P_{\mathrm{C-O}}(t) = \exp\left[-\left(\frac{t}{\tau_{\mathrm{KWW}}}\right)^{\beta}\right] \tag{9}$$

with $\beta = 0.311$ and $\tau_{\mathrm{KWW}} = 1196$ ps. The time integral of eq 9 provides the autocorrelation time τ for a non-Debye process.

In the case of OACF for C−O vectors, we find $\tau = 6.8 \pm 0.2$ ns by integration of the KWW fit in a time range of 0−100 ns. The τ value, indicating the time scale for a complete rotational decorrelation of C−O vectors in the PVA network, is about 40 times the average rotational lifetime $<\tau_{\mathrm{rot}}>$, not surprising evidence if you consider that the complete rotational decorrelation of the single C−O vector probably occurred as a result of many cooperative transitions of neighboring dihedrals.

Tamai and Tanaka report a orientational relaxation time of about 7 ns for the C−C vector of PVA in a MD investigation of a 50% (w/w) aqueous solution of a PVA polymer chain with a polymerization degree of 81 at 300 K.[32] This value, similar to that found for C−O vectors in the present work, suggests that the presence of chemical junctions in a PVA telechelic network with $\Phi_2 = 0.12$ does not alter the dynamics of the chain reorientation process.

It is interesting to compare our results with data obtained in a MD study of poly(ethylene oxide) PEO aqueous solutions at 313 K.[30] For C−H vectors in PEO chains with a 12 repeat unit, Smith et al.[30] find orientational autocorrelation times about 2 order of magnitude lower than our result. A determining contribution to this remarkable difference between PVA and PEO can be ascribed to the different polymer−water interaction. Unlike PEO, PVA hydroxylic groups are involved in HB interactions with water molecules both as donors and acceptors and have a side-chain location that is more accessible that that of PEO oxygen atoms. These chemical and structural characteristics give rise to a strong interaction of PVA with water, influencing the dynamics both of the water itself and of the polymer.

The chain dynamics could be affected by intramolecular interactions, such as hydrogen bonding between hydroxylic groups of different PVA residues. Figure 8 shows the number of intramolecular HBs per PVA residue as a function of time and the corresponding time autocorrelation function $C_{\mathrm{HB}}(t)$ (inset). The modulation in the HB number, observed in Figure 8 at about 3100 ps, is related to a rearrangement toward a coiled conformation of part of a network chain. About four HBs per every ten PVA repeat units are found on average, in agreement with the findings of Müller-Plathe at al.[33] and Tamai et al.[50]

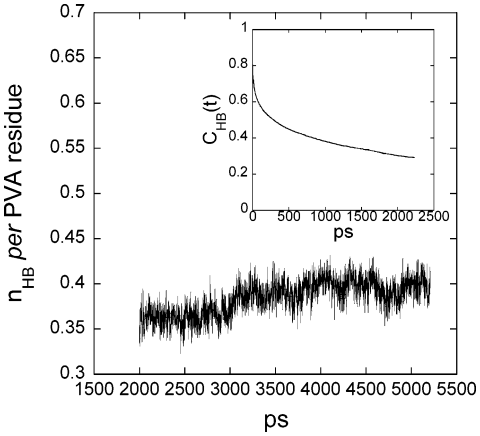

Figure 8. Number of PVA intramolecular HBs per PVA residue as a function of time. Inset: decay of the HB autocorrelation function $C_{HB}(t)$ between PVA hydroxylic groups.

for PVA aqueous solutions at 300 K. The total autocorrelation time, evaluated by the time integral of the $C_{HB}(t)$ fitted to eq 9 with $\beta = 0.261$ and $\tau_{KWW} = 1108$ ps in an interval of 0−100 ns, is 9 ± 3 ns. The last value provides an estimate of the order of magnitude of the lifetime of these interactions and represents the necessary time in order that all the particular intramolecular HBs are definitely interrupted in the trajectory. Considering that HBs between OH groups of topologically distant residues have been found in the simulation for the occurrence of loops and entanglements, the intramolecular HB autocorrelation time refers to a time scale involving dynamical events of a large part of the network.

3.3. Network Properties. Chain density in the dry system, ν, number-average molecular weight of the network chains, M_c, and mesh size, ξ, are characteristic parameters of a polymer network. ν and M_c can be experimentally determined by dynamic mechanical analysis. An evaluation of ξ is usually performed, knowing M_c, by means of eq 10

$$\xi = \frac{(C_n n)^{1/2} l}{\Phi_2^{1/3}} \tag{10}$$

where C_n, l, and Φ_2 are the characteristic ratio, the residue length, and the volume fraction of the polymer, respectively, and n is the DP corresponding to M_c. Equation 10 derives by a coarse representation of the network where pores and chains with the same geometry and a Gaussian behavior of the polymer chains have been assumed and provides an estimate of the network porosity.

In our simulation, only M_c and Φ_2 (by fixing topology and water content) have been imposed in the building of the hydrogel model, according to experimental results. The chain density in the swollen hydrogel, ρ_h, of 5×10^{-5} mol/cm^3 used in the simulation has been established after equilibrium is reached, a value in good agreement with the experimental of 4.4×10^{-5} mol/cm^3, given as

$$\rho_h = \nu \cdot \Phi_2 \tag{11}$$

An average mesh size of 7 ± 1 nm has been experimentally evaluated by eq 10 for telechelic PVA hydrogel systems modeled in the present work.[36] A comparison of this ξ value with the simulation results has been performed by monitoring the time behavior of the three vectors defined in the simulation box by connecting opposite junction points of the network mesh. The absolute values of the mesh vectors throughout the trajectory, reported in Figure 9, range from about 3 to 5 nm, in satisfactory agreement with the experimental estimate of the network porosity by considering the simplicity of the model. The local heterogeneity of the polymer scaffold, indicated in Figure 9 by the different average values of the three lengths on the time scale of our simulation, is not surprising by considering that long-range relaxations of complex polymer systems occur in a time domain of microseconds,[25] not accessible at the present to MD simulations with atomic detail. In addition, we have examined the end-to-end distance and the radius of gyration R_g of the network chains, and average values are given in Table 3. The ratio of end-to-end distance and R_g provides a criterion to evaluate the conformational behavior of a polymer chain since, for a Gaussian polymer chain, this ratio is equal to $\sqrt{6} \sim 2.4$. The values of the ratios reported in Table 3 are well below the Gaussian value for the chains between junctions, constituted by 67 repeating units, indicating that the DP is too small to allow a random walk behavior. A Gaussian character is shown by the three percolating chains (A, B, C in Chart 1 and Table 3), each of 138 residues, with an average value of 2.5 for the ratio of the end-to-end distance and R_g. The characteristic ratio of A, B, C chains in the simulation is 6.8, in reasonable agreement with the value of 8.3,[51] obtained for PVA aqueous solutions at 30 °C.

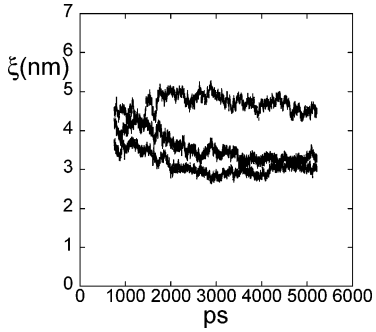

Figure 9. Absolute values of the mesh vectors as a function of time.

TABLE 3: End-to-End Distance and Radius of Gyration of PVA Chains in the Network[a]

chain	end-to-end distance (nm)	R_g(nm)	end-to-end distance/R_g
A*[b]	2.6 (0.1)	1.40 (0.04)	1.9
B*[b]	4.3 (0.4)	2.15 (0.05)	2.0
C*[b]	2.4 (0.1)	1.71 (0.04)	1.4
D[b]	2.7 (0.1)	1.90 (0.06)	1.4
E[b]	2.6 (0.2)	1.45 (0.03)	1.8
F[b]	2.7 (0.2)	1.17 (0.04)	2.3
A[c]	6.7[d]	2.32 (0.02)	2.9
B[c]	6.7[d]	2.96 (0.06)	2.3
C[c]	6.7[d]	2.64 (0.05)	2.4

[a] Standard deviation in parentheses. [b] Polymer chain between near-neighbor junctions. [c] Whole percolating chain (see Chart 1). [d] Box size.

4. Concluding Remarks

In the present work, we have developed a realistic model of a PVA chemical hydrogel at a high hydration degree for an all-atom MD study. The analysis of the trajectory in a time interval of 5 ns allowed us to characterize the polymer−water interaction and the segmental dynamics of PVA in the network and to evaluate the supercooling effect on water in the hydrogel.

Our results seem to indicate that the interaction with solvent governs the local chain dynamics and that the topological constraints of chemical junctions, at the investigated cross-

linking density, are not relevant for the local mobility. The characteristic conformational transition times are in agreement with residence times of the polymer confined motion obtained by QENS experiments. The water diffusion behavior is also affected by interaction with PVA, with a slowing effect that involves about 30% of the solvent in the hydrogel.

The results of the analysis of network structural parameters in this simulation give confidence to the model used for the study of water dynamics and local polymer mobility. An investigation of the scaffold dynamics on larger space and time domain is beyond the objectives of the present work. Neutron spin-echo experiments are forecast to characterize the network dynamics in a time window of hundreds of nanoseconds.

Acknowledgment. We gratefully acknowledge Dr. M. Sega for helpful discussions and INSTM/CINECA for partial financial support.

References and Notes

(1) Zhang, L.-M.; Zhou, Y.-J.; Wang, Y. *J. Chem. Technol. Biotechnol.* **2006**, *81*, 799.
(2) Kang, H. G.; Lee, S. B.; Lee, Y. M. *Polym. Int.* **2005**, *54*, 537.
(3) Wu, W.; Li, W.; Wang, L. Q.; Tu, K.; Sun, W. *Polym. Int.* **2006**, *55*, 513.
(4) Ng, L.-T.; Swami, S. *Polym. Int.* **2006**, *55*, 535.
(5) Maleki, A.; Kjoniksen, A. L.; Knudsen, K. D.; Nystrom, B. *Polym. Int.* **2006**, *55*, 565.
(6) El-Rehim, H.; Hegazy, El-Sayed.; Diaa, D. *J. Macromol. Sci., Pure Appl. Chem.* **2005**, *43*, 101.
(7) Xiong, J.-Y.; Narayanan, J.; Liu, X.-Y.; Chong, T. K.; Chen, S. B.; Chung, T.-S. *J. Phys. Chem. B* **2005**, *109*, 5638.
(8) Pastoriza, A.; Pacios, I. E.; Piérola, I. F. *Polym. Int.* **2005**, *54*, 1205.
(9) Podual, K.; Peppas, N. A. *Polym. Int.* **2005**, *54*, 581.
(10) Chowdhury, M. A.; Hill, D. J. T.; Whittaker, A. K. *Polym. Int.* **2005**, *54*, 267.
(11) Zhang, X.-Z.; Sun, G.-M.; Wu, D.-Q.; Chu, C.-C. *J. Mater. Sci.: Mater. Med.* **2004**, *15*, 865.
(12) Anrather, D.; Smetazko, M.; Saba, M.; Alguel, Y.; Schalkhammer, T. *J. Nanosci. Nanotechnol.* **2004**, *4*, 1.
(13) Eddington, D. T.; Beebe, D. J. *Adv. Drug Delivery Rev.* **2004**, *56*, 199.
(14) Petrova, R. I.; Swift, J. A. *J. Am. Chem. Soc.* **2004**, *126*, 1168.
(15) Bajpai, A. K.; Giri, A. *React. Funct. Polym.* **2002**, *53*, 125.
(16) Caseli, L.; Zaniquelli, M. E. D.; Furriel, R. P. M.; Leone, F. A. *Colloids Surf., B* **2002**, *25*, 119.
(17) Galantini, L.; D'Archivio, A. A.; Lora, S.; Corain, B. *J. Mol. Catal. B: Enzym.* **1999**, *6*, 505.
(18) Trevors, J. T.; Pollack, G. H. *Prog. Biophys. Mol. Biol.* **2005**, *89*, 1.
(19) Paradossi, G.; Cavalieri, F.; Chiessi, E. *Curr. Pharm. Des.* **2006**, *12*, 1403.
(20) Tsang, V. L.; Bhatia, S. N. *Adv. Drug Delivery Rev.* **2004**, *56*, 1635.
(21) Landers, R.; Hubner, U.; Schmelzeisen, R.; Mulhaupt, R. *Biomaterials* **2002**, *23*, 4437.
(22) Plumridge, T. H.; Waigh, R. D. *J. Pharm. Pharmacol.* **2002**, *54*, 1155.
(23) *Hydrogels and Biodegradable Polymers for Bioapplications*; Ottenbrite, R. M., Huang, S. J., Park, K., Eds.; American Chemical Society: Washington, DC, 1996.
(24) Creighton, T. E. *Curr. Biol.* **1997**, *7*, R380.
(25) Karayiannis, N. Ch.; Mavrantzas, V. G. *Macromolecules* **2005**, *38*, 8583.
(26) Vasilevskaya, V. V.; Khalatur, P. G.; Khokhlov, A. R. *Macromolecules* **2003**, *36*, 10103.
(27) Kenkare, N. R.; Smith, S. W.; Hall, C. K.; Khan, S. A. *Macromolecules* **1998**, *31*, 5861.
(28) Ivanov, I.; Vemparala, S.; Pophristic, V.; Kuroda, K.; DeGrado, W. F.; McCammon, J. A.; Klein, M. L. *J. Am. Chem. Soc.* **2006**, *128*, 1778.
(29) Sun, Q.; Faller, R. *J. Phys. Chem. B* **2005**, *109*, 15714.
(30) Borodin, O.; Bedrov, D.; Smith, G. D. *Macromolecules* **2001**, *34*, 5687.
(31) Tamai, T.; Tanaka, H. *Chem. Phys. Lett.* **1998**, *285*, 127.
(32) Tamai, T.; Tanaka, H. *Fluid Phase Equilib.* **1998**, *144*, 441.
(33) Müller-Plathe, F.; van Gunsteren, W. F. *Polymer* **1997**, *38*, 2259.
(34) Netz, P. A.; Dorfmüller, T. *J. Phys. Chem. B* **1998**, *102*, 4875.
(35) Longhi, G.; Lebon, F.; Abbate, S.; Fornili, S. L. *Chem. Phys. Lett.* **2004**, *386*, 123.
(36) Paradossi, G.; Cavalieri, F.; Chiessi, E.; Telling, M. T. F. *J. Phys. Chem. B* **2003**, *107*, 8363.
(37) Chiessi, E.; Cavalieri, F.; Paradossi, G. *J. Phys. Chem. B* **2005**, *109*, 8091.
(38) Cavalieri, F.; El Hamassi, A.; Chiessi, E.; Paradossi, G.; Villa, R.; Zaffaroni, N. *Biomacromolecules* **2006**, *7*, 604.
(39) Cavalieri, F.; El Hamassi, A.; Chiessi, E.; Paradossi, G. *Langmuir* **2005**, *21*, 8758.
(40) Paradossi, G.; Cavalieri, F.; Chiessi, E.; Ponassi, V.; Martorana, V. *Biomacromolecules* **2002**, *3*, 1255.
(41) Berendsen, H. J. C.; Postma, J. P. M.; van Gunsteren, W. F.; Hermans, J. In *Intermolecular Forces*; Pullman, B., Ed; Reidel: Dordrecht, The Netherlands, 1981; p 239.
(42) Berendsen, H. J. C.; van der Spoel, D.; van Drunen, R. *Comput. Phys. Commun.* **1995**, *91*, 43.
(43) Lindahl, E.; Hess, B.; van der Spoel, D. *J. Mol. Model.* **2001**, *7*, 306.
(44) Hockney, R. W.; Goel, S. P. *J. Comput. Phys.* **1974**, *14*, 148.
(45) Berendsen, H. J. C.; Postma, J. P. M.; van Gunsteren, W. F.; DiNola, A.; Haak, J. R. *J. Chem. Phys.* **1984**, *81*, 3684.
(46) de Moura, A. F.; Trsic, M. *J. Phys. Chem. B* **2005**, *109*, 4032.
(47) Peppas, N. A.; Merril, E. W. *J. Polym. Sci.* **1976**, *14*, 459. Peppas, N. A.; Benner, R. E., Jr *Biomaterials* **1980**, *1*, 158.
(48) Krynicki, K.; Green, C. D.; Sawyer, D. W. *Faraday Discuss. Chem. Soc.* **1978**, 199.
(49) Texeira, J.; Bellisent-Funel, M. C.; Chen, S. H.; Dianoux, A. J. *Phys. Rev. A* **1985**, *31*, 1913.
(50) Tamai, T.; Tanaka, H.; Nakanishi, K. *Mol. Simul.* **1996**, *16*, 359.
(51) *Polymer Handbook*, 4th ed., Brandrup, J., Immergut, E. H., Grulke, E. A. Eds.; John Wiley & Sons, New York, 1999.